




Stimuli-responsive polymersomes of poly [2-(dimethylamino) ethyl methacrylate]-*b*-polystyrene

Valdomiro V. de Souza¹ · Gustavo P. B. Carretero¹ · Phelipe A. M. Vitale¹ · Íris Todeschini³ · Paloma O. Kotani¹ · Greice K. V. Saraiva¹ · Cristiane R. Guzzo³ · Hernan Chaimovich¹ · Fabio H. Florenzano²  · Iolanda M. Cuccovia¹

Received: 25 August 2020 / Revised: 20 November 2020 / Accepted: 29 December 2020 /
Published online: 12 January 2021

© The Author(s), under exclusive licence to Springer-Verlag GmbH, DE part of Springer Nature 2021

Abstract

Amphiphilic diblock copolymers may assemble in aqueous solutions to form vesicles delimited by a polymeric double layer, also known as polymersomes, considered a more robust option to liposomes. Diblock copolymers may respond to pH, temperature, and other conditions. Because of such properties, polymersomes are currently being studied as drug delivery systems or as nanoreactors. pH-responsive polymersomes are potentially crucial because unusual pH gradients are present in cells under several physiological and pathological conditions. We synthesized two diblock copolymers of poly [2-(dimethylamino) ethyl methacrylate]-*block*-polystyrene (PDMAEMA-*b*-PS) via RAFT. We both developed new materials and better-understood polymersomes' properties with pH and temperature-responsive groups with these polymers. GPC, ¹H-NMR, and FTIR characterized copolymers. The ionization equilibrium of the PDMAEMA amino groups on the polymersomes was analyzed by potentiometric titration and Zeta potential measurements. The hydrodynamic radius of the polymersomes in different pH and temperatures was analyzed by DLS. Entrapment of an electron paramagnetic resonance probe indicated the presence of a hydrophilic inner core. Negative staining transmission electron microscopy showed spherical aggregates and confirmed the diameter around 80 nm. These polymersomes with dual stimulus–response (i.e., pH and temperature) may be a platform for gene delivery and nanoreactors.

Keywords Polymersome · RAFT · PDMAEMA-*b*-polystyrene · LCST

✉ Fabio H. Florenzano
fhfloren@usp.br

¹ Department of Biochemistry, Institute of Chemistry, University of São Paulo, São Paulo 05508-000, Brazil

² Department of Materials Engineering, Engineering School of Lorena, University of São Paulo, Lorena 12602-810, Brazil

³ Department of Microbiology, Institute of Biomedical Sciences, University of São Paulo (USP), São Paulo 05508-900, Brazil

Introduction

Polymersomes, or polymer vesicles, are nanometer-sized spheroidal aggregates that, in water, present an aqueous internal compartment, external and internal hydrophilic coronas, and a hydrophobic membrane-like structure separating the coronas [1].

Polymersomes have gained considerable interest due to their potential applications in drug delivery, gene therapy, theranostics, artificial organelles, and nanoreactors [2–7]. Polymersomes are, in general, more stable and robust than liposomes and can respond to external stimuli [5, 8]. Interest in polymersomes' pH responsiveness is significant since pH gradients are typical in several physiological and pathological conditions [3–5, 9–13]. Due to their broad range of applications, it is interesting to develop easy-to-obtain polymersomes that exhibit responses to external conditions changes [1, 3, 6, 14, 15].

As amphiphilic diblock copolymers may self-assemble in water, they can form polymersomes with potential applications in medical, biological, and chemical sciences [6, 16–19]. Amphiphilic diblock copolymers have a hydrophilic and a hydrophobic block. A block copolymer bearing poly [2-(dimethylamino) ethyl methacrylate] (PDMAEMA) as the hydrophilic block and polystyrene (PS) as the hydrophobic block (Fig. 1) forms aggregates that precipitate at higher temperatures due to the low critical solution temperature (LCST) of the PDMAEMA block. The temperature at which the polymersomes become water-incompatible is strongly pH dependent. Hence, these systems are both pH- and temperature responsive [7, 19–28].

Genes [29] or gene/drugs [30] can be delivered using PDMAEMA and derived copolymers. PDMAEMA side chain amino groups undergo protonation/deprotonation equilibrium, so negatively charged molecules like DNA can bind, mainly when the protonated form of the polymer predominates. Biological compartments such as the interior of cell organelles present pH variations so that the electrostatic bound may be weakened in higher pH, releasing the attached molecule—DNA, for example—in a site of interest. That is a strategy to target a molecule (drug or nucleic acid) to specific locations inside the cell [3]. Supramolecular aggregates such as polymersomes containing PDMAEMA-based polymers may improve the delivery

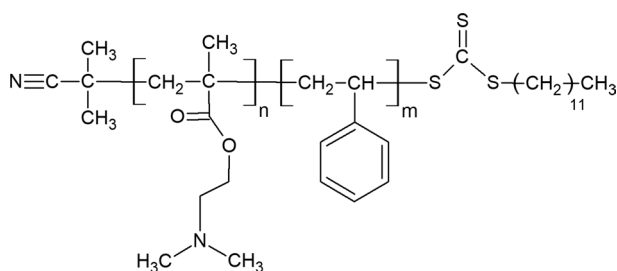


Fig. 1 General structure of diblock copolymers PDMAEMA_n-*b*-PS_m, obtained by the RAFT technique. *m* and *n* are the numbers of styrene and DMAEMA units, respectively. The end-groups are typical of a RAFT-made polymer with the specific CTA used in this work. The amine group on the DMAEMA unit is responsible for the pH-response of the copolymers in aqueous media

properties of systems designed to carry genes or drugs; therefore, the deep understanding of their properties is of great interest, including the protonation equilibrium process on the polymersome surface.

Reversible deactivation radical polymerization (RDRP) techniques allowed the production of polymers with precise architecture and composition. Advances of RDRP are crucial to the synthesis of diblock copolymers tailored to assemble in water in various types of aggregates, including polymersomes, because they allow the synthesis of a homopolymer block that can be further extended with a different monomer, resulting in a diblock copolymer [5, 7, 28, 31–39]. Therefore, RDRP techniques are crucial to the development of new routes to synthesize functional block copolymers such as PDMAEMA-*b*-PS [28], used in this work.

The RDRP variant known as reversible addition-fragmentation chain transfer (RAFT) polymerization is useful to generate amphiphilic diblock copolymers prone to assemble into polymersomes [31]. In this work, we synthesized two different diblock copolymers (PDMAEMA-*b*-PS) by RAFT and assembled polymersomes in aqueous solutions. This system's in-depth characterization is presented, including average size, size distribution, surface charge density, and probing of the internal aqueous compartment.

Experimental

Materials

Deuterated chloroform (CDCl_3), deuterated water (D_2O), dimethyl-2-(aminoethyl) methacrylate (DMAEMA, 98%) and styrene (98%) were from Sigma-Aldrich. Monomers stabilizer was removed by De-HiBit-200 (Polysciences, Inc.). NaH_2PO_4 , HCl and NaOH were from Merck. 2,2'-azobis-isobutyronitrile (AIBN), 1,1'-Azobis(cyclohexanecarbonitrile) (ACHN), and the chain transfer agent (CTA) 2-Cyano-2-propyl dodecyl trithiocarbonate were from Sigma-Aldrich and used as received. Milli Q (Millipore Co.) purified water was used throughout. The spin probe 4-trimethylammonium-2,2,6,6-tetramethylpiperidine-1-oxyl iodide (CAT1) was obtained from Fisher Scientific. Tetrahydrofuran (THF) (HPLC grade) was from J.T. Baker. All other chemicals were of analytical grade, obtained from Sigma-Aldrich and used without purification.

RAFT polymerization synthesis of amphiphilic diblock copolymers of PDMAEMA_n-*b*-PS_m

The materials used to assemble into polymersomes were synthesized via RAFT. Two PDMAEMA_n-*b*-PS_m copolymers bearing the same PDMAEMA block were used. Briefly, a PDMAEMA_nmacroCTA was first synthesized, in bulk, using 2-cyano-2-propyl dodecyl trithiocarbonate as chain transfer agent (CTA) and ACHN as initiator. The PDMAEMA_nmacroCTA-homopolymer was purified by several dissolution/precipitation cycles in THF and methanol. As the aim of

this synthesis was macroCTA, the relatively high M_w/M_n (1.65, Table 1) of the product was considered acceptable for further use. Purified macroCTA was used to synthesize, in bulk, two PDMAEMA-*b*-PS with different PS block lengths (PDMAEMA₃₁₅-*b*-PS₂₄₄ and PDMAEMA₃₁₅-*b*-PS₇₈₁) with AIBN as initiator. The two copolymers obtained were isolated by precipitation in hexane (from THF solutions) and dried for 2 days at 40 °C. All syntheses were performed in argon atmosphere and under 600 rpm magnetic stirring.

Characterization of amphiphilic diblock copolymers of PDMAEMA_n-*b*-PS_m

GPC

Gel permeation chromatographic (GPC/SEC) was used to determine the average molar masses of the PDMAEMA macroCTA and of the copolymers [40] on a GPC Shimadzu Prominence series equipped with a pre-column Phenogel, 5 μm, and two columns in series: Phenogel 5 μm, 1×10^6 Å and 5 μm, 1×10^4 Å (Phenom-enex). The injected volume of the sample was 10 μL (10 mg mL⁻¹), and the analysis was performed at 35 °C. A differential refractive index detector (Shimadzu RID-10A) was used. The mobile phase was THF with triethylamine 0.3% at a flow rate of 0.8 mL min⁻¹. The system was calibrated with polymethylmethacrylate (PMMA) (EasyCal, Sigma-Aldrich) standards ($M_p \sim 800$ – $2,000,000$ g mol⁻¹). The polymer chains molar mass progression of all syntheses was monitored by GPC analysis of the aliquots taken at different reaction times.

Nuclear magnetic resonance (NMR)

Copolymer chemical structure and PDMAEMA/PS ratios were determined by ¹H-NMR spectra using a Varian (Mercury model) spectrometer operating at 300 MHz (¹H frequency). The spectra were recorded at room temperature in CDCl₃ (10 mg mL⁻¹) and were obtained with 90° pulses of 8.0 μs and a spectral window of 12 ppm. ¹H-NMR chemical shift assignments of all materials were in agreement with the literature [7, 41, 42].

Table 1 Synthesis parameters and characterization data of the polymers [PDMAEMA_n-*b*-PS_m]

Material	n:m ^a	M_n^b (kg mol ⁻¹)	M_w^b/M_n
PDMAEMA ₃₁₅ macroCTA	–	54.7	1.65
PDMAEMA ₃₁₅ - <i>b</i> -PS ₂₄₄	1:0.775	74.8	1.56
PDMAEMA ₃₁₅ - <i>b</i> -PS ₇₈₁	1:2.48	145	1.49

^an/m ratios (PDMAEMA (*n*) and polystyrene (*m*)) were calculated from the areas under the ¹H NMR peaks and GPC total molar mass (see "Methods")

^bData obtained by GPC

Fourier Transform Infrared Spectroscopy (FTIR)

Fourier transform infrared spectroscopy (FTIR) analysis was used to confirm the copolymer molecular structure and to prove the purity of the synthesized polymers. Measurements were performed on IR Prestige 21 spectrometer (Shimadzu) using ATR mode.

Titration

The pK_a of the amino groups of the copolymers were determined potentiometrically in a DIGIMED DM-20 pH meter (São Paulo, Brazil) equipped with a semi-micro-combination electrode (Corning, USA) in N_2 atmosphere as described by Saraiva et al. [43]. The copolymers were solubilized in THF, maintained under stirring for 2 h and, after solubilization, kept in a refrigerator overnight. The stock solutions of PDMAEMA₃₁₅-*b*-PS₂₄₄ and PDMAEMA₃₁₅-*b*-PS₇₈₁ were 0.02538 g mL⁻¹ and 0.05135 g mL⁻¹, respectively. Copolymer concentrations were calculated to yield the same moles of amine groups in both experiments. For PDMAEMA₃₁₅-*b*-PS₂₄₄ titration, 0.12 mL of the solution was added to 30 mL of HCl 0.0025 M, pH 2.45, under vigorous stirring and the titration was performed with NaOH 0.05 M. For PDMAEMA₃₁₅-*b*-PS₇₈₁, 0.06 mL of the stock solution was used. The HCl 0.0025 M, pH 2.45, solution was previously titrated with the same NaOH solution.

Assembly of polymersomes in aqueous solution

Polymersomes based on copolymers of DMAEMA and PS were prepared via solvent switch [41, 44]. The two amphiphilic block copolymers were dissolved in tetrahydrofuran (THF) to a final concentration of 40 mg mL⁻¹. Subsequently, in a flask containing 2 mL of Tris–HCl buffer 10 mmol L⁻¹, pH 7.4, under stirring at 1000 rpm, 50 μ L of the copolymers in THF was slowly added for the assembly of the polymersomes in the final concentration of 1 mg mL⁻¹. Polymersomes were prepared at room temperature, and the final THF content was 2.5% (v/v).

Determination of the aqueous internal volume of polymersomes—Encapsulation of CAT1 probe measured by electronic paramagnetic resonance (EPR)

Spectra were obtained in a Bruker EMX-200 spectrometer (Bruker, Germany) using trimethylammonium-2,2,6,6-tetramethylpiperidine-1-oxyl iodide (CAT1) as probe [45].

Polymersomes were prepared by injecting 50 μ L of each copolymer solution (at concentration of 40 mg mL⁻¹ of copolymer in THF) to 2 mL of Tris–HCl buffer 10 mmol L⁻¹, pH 7.4, containing 1.5 mmol L⁻¹ of CAT1 spin probe, to a final concentration of 13.4 μ mol L⁻¹ of PDMAEMA₃₁₅-*b*-PS₂₄₄ and 6.9 μ mol L⁻¹ of PDMAEMA₃₁₅-*b*-PS₇₈₁.

EPR signal of 170 μL of the sample, placed in flat quartz cells (Wilmad, USA), was measured before and after the addition of 10 μL of a 0.04 mol L^{-1} of ascorbic acid solution freshly prepared, to a final concentration of 2.35 mmol L^{-1} of ascorbic acid. The CAT1 signal is suppressed by an oxidation–reduction reaction with the ascorbic acid. The ratio between the signal before (total signal) and after (residual signal) suppression adjusted for the dilution was used to calculate the percentage of encapsulated probe and the total internal volume of the aqueous compartments inside the polymersomes (Eq. 1) [46].

$$\% \text{Entrapment} = 100 * \text{Residual signal} / \text{Total signal} = 100 * \text{Internal volume} / 170 \mu\text{L} \quad (1)$$

The % of entrapment and internal aqueous volume was analyzed as a function of the final polymer concentration in the sample. Control samples to test the signal suppression reaction consisted of the CAT1 solution in buffer without the polymers in which ascorbic acid was added at the same proportion of the sample containing the polymersomes.

Dynamic Light Scattering (DLS)

The hydrodynamic diameter (D_h) and the surface charge density (Zeta potential) of the polymersomes were measured by dynamic light scattering (DLS) using a Zeta-sizer Nano 317 (Malvern) at 25 °C. Buffers were previously filtered through Millipore Millex LCR (0.22 μm) and the copolymer solutions in THF through Millipore PTFE filters (0.45 μm). The concentration of all buffers was 0.01 mol L^{-1} . The average size of the polymersomes prepared in different buffers was studied at different temperatures ranging from 25 to 85 °C to verify thermal transitions such as LCST and the conditions in what the transition takes place. Hydrodynamic diameter data are expressed both as size scatter average (calculated averaging the total scattered light intensity as function of size, Fig. 5) and as size number average (calculated from the total scattered light normalized by each related size, Table 2). Size scatter

Table 2 Hydrodynamic diameter (number average, nm), polydispersity index (PdI) and zeta potential (mV) values of polymersomes of PDMAEMA₃₁₅-*b*-PS₂₄₄ and PDMAEMA₃₁₅-*b*-PS₈₇₁, with the respective standard deviations (SD), in different buffers (0.01 mol L^{-1}) and pHs. All experiments were performed at 25 °C

Buffer	pH	Diameter (number average, nm) (SD)	PdI (SD)	Zeta potential (mV) (SD)
PDMAEMA ₃₁₅ - <i>b</i> -PS ₂₄₄				
Acetate	5.0	96 (6)	0.64 (0.20)	+44.2 (1.9)
Tris–HCl	7.4	147 (25)	0.71 (0.24)	+29.3 (3.9)
Tris–HCl	8.0	86 (26)	0.54 (0.06)	+25.0 (2.4)
Phosphate	8.0	93 (9)	0.45 (0.05)	+12.8 (1.0)
PDMAEMA ₃₁₅ - <i>b</i> -PS ₇₈₁				
Acetate	5.0	104 (18)	0.46 (0.02)	+43.0 (1.0)
Tris–HCl	7.4	80 (20)	0.36 (0.08)	+33.5 (1.2)
Tris–HCl	8.0	58 (3)	0.29 (0.06)	+20.9 (2.1)
Phosphate	8.0	111 (19)	0.29 (0.11)	+12.6 (0.5)

average is used to monitor overall changes in the size distribution of the sample as temperature was increased, while size number average values report the size distribution in terms of number of particles at each size. All data are the mean of triplicate measurements \pm SD.

Analyzes of polymersomes by negative staining transmission electron microscopy (TEM)

TEM was performed using a FEI Tecnai G20 200 kV transmission electron microscope, at the Institute of Biomedical Sciences (ICB) of University of São Paulo (USP). A grid, 400 mesh of a carbon thin layer film (Electron Microscopy Sciences), was negatively glow-discharged for 15 s at plasma current of 14 mA. Then, the grid was added to the top of a drop of 20 μ L of polymersomes at the concentration of 2.5 mg mL⁻¹ for 2 min followed by two rinses using water. The grid containing the sample was put at the top of a 2% uranyl acetate drop for 2 min, followed by drying using a filter paper and left to dry at room temperature. The images were then obtained, and visualization, selection and analysis were performed using ImageJ program.

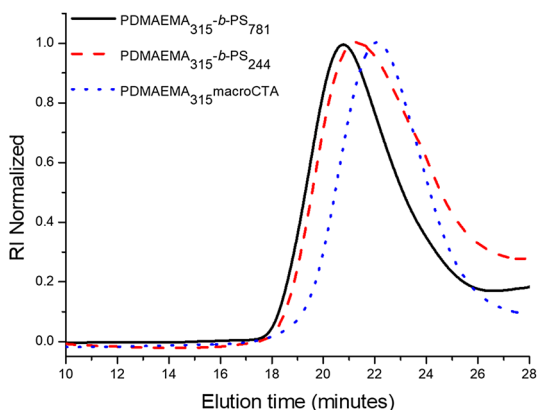
Results and discussion

Polymer synthesis and characterization

Figure 2 shows typical GPC (see "Methods" section) traces of the polymers. Copolymers showed only one signal throughout the polymerization, indicating that PDMAEMA chains were extended. As the total average molar masses were determined by GPC using PMMA standards, the molar mass units in Table 1 refer to PMMA molar mass/hydrodynamic relationship.

Characterization data of the polymers are described in Table 1. The molar mass dispersities (M_w/M_n) below 1.5 are characteristic of controlled radical

Fig. 2 GPC elution profiles of PDMAEMA₃₁₅-*b*-PS₇₈₁, PDMAEMA₃₁₅-*b*-PS₂₄₄, and PDMAEMA₃₁₅macroCTA. The mobile phase was THF with triethylamine 0.3% at a flow rate of 0.8 mL.min⁻¹



polymerizations [34]. The results presented here are around or higher than that. Even though this finding points out to some lack of polymerization control, RAFT was used here in order to solely facilitate the generation of block copolymers. That goal was accomplished, as demonstrated by GPC, FTIR and NMR, so the relatively high values of M_w/M_n are not relevant in this context. As mentioned previously, all PDMAEMA macroCTA chains were extended during the copolymerization, so is very likely that all of them carried the RAFT agent functionality before PS elongation.

The hydrophilic (n) and hydrophobic (m) blocks ratios (Fig. 1, Table 1) and the copolymer average formula [PDMAEMA $_n$ - b -PS $_m$] were calculated combining the total molar masses (GPC data) and the data obtained by $^1\text{H-NMR}$ (Fig. 3).

PDMAEMA/PS ratios (n/m ratio) of the copolymers were calculated from the areas under the $^1\text{H-NMR}$ signals corresponding to the side chain methylene group of the ester in the PDMAEMA unit ($-\text{O}-\text{CH}_2-$) (n), and the aromatic protons of the PS block (m) according to Eq. 2:

$$n_{(\text{PDMAEMA})}/m_{(\text{PS})} = (A_d * 5)/(A_c * 2) \quad (2)$$

In Eq. 2, A_d represents the area under the methylene groups peak of PDMAEMA and A_c is the area under the peak of the aromatic protons of PS. The coefficients 5 and 2 normalized the areas for the number of hydrogens from the methylene of DMAEMA and the aromatic ring of PS, respectively. The indexes n and m are the number of units of DMAEMA and PS, respectively, in the copolymer chains. The total polymer mass, M_n , is given by the relative composition of the two monomers as described in Eq. 3:

$$M_n = n * (\text{PDMAEMA}) + m * (\text{PS}) \quad (3)$$

where (PDMAEMA) and (PS) are the monomer molecular masses, i.e., 157.9 and 104 $\text{g}\cdot\text{mol}^{-1}$, respectively. M_n was obtained by GPC analysis.

All spectra exhibit the $^1\text{H-NMR}$ peaks at 0.6, 2.3, 2.6, and 4.1 ppm, characteristics of the PDMAEMA block (Fig. 3a–c). The $^1\text{H-NMR}$ peaks of the aromatic hydrogens in the PS block of the copolymers were between 6.5 and 7.5 ppm in copolymers PDMAEMA $_{315}$ - b -PS $_{244}$ and PDMAEMA $_{315}$ - b -PS $_{781}$ (Fig. 3b, c) [47].

In the FTIR spectra of both PDMAEMA $_{315}$ - b -PS $_{244}$ and PDMAEMA $_{315}$ - b -PS $_{781}$, strong signals at 698 cm^{-1} related to out-of-plane angular deformation relative to the aromatic rings of the styrene structure were evident (Fig. 3b, c) [48], demonstrating effective copolymerization. Additionally, the C-H stretching signals near 3030 cm^{-1} , characteristic of aromatic C-H bonds [49], were also evident in the copolymer spectra (Fig. 3). The expected PDMAEMA carbonyl ester stretching signal at 1725 cm^{-1} is present in all spectra, a clear evidence of the presence of the block [50].

The pH-dependent protonation/deprotonation of PDMAEMA alters the hydrophilic/hydrophobic balance of the corresponding copolymers determining the morphology and the size of the self-assembled structures [20, 21, 25, 37, 51–54]. The pKa of the DMAEMA monomer is ca. 8.3 [22, 23, 55–57]. Titrations of PDMAEMA $_{315}$ - b -PS $_{244}$ and PDMAEMA $_{315}$ - b -PS $_{781}$ exhibited two endpoints (Fig. 4): the first one corresponding to the titration of the excess HCl and the second

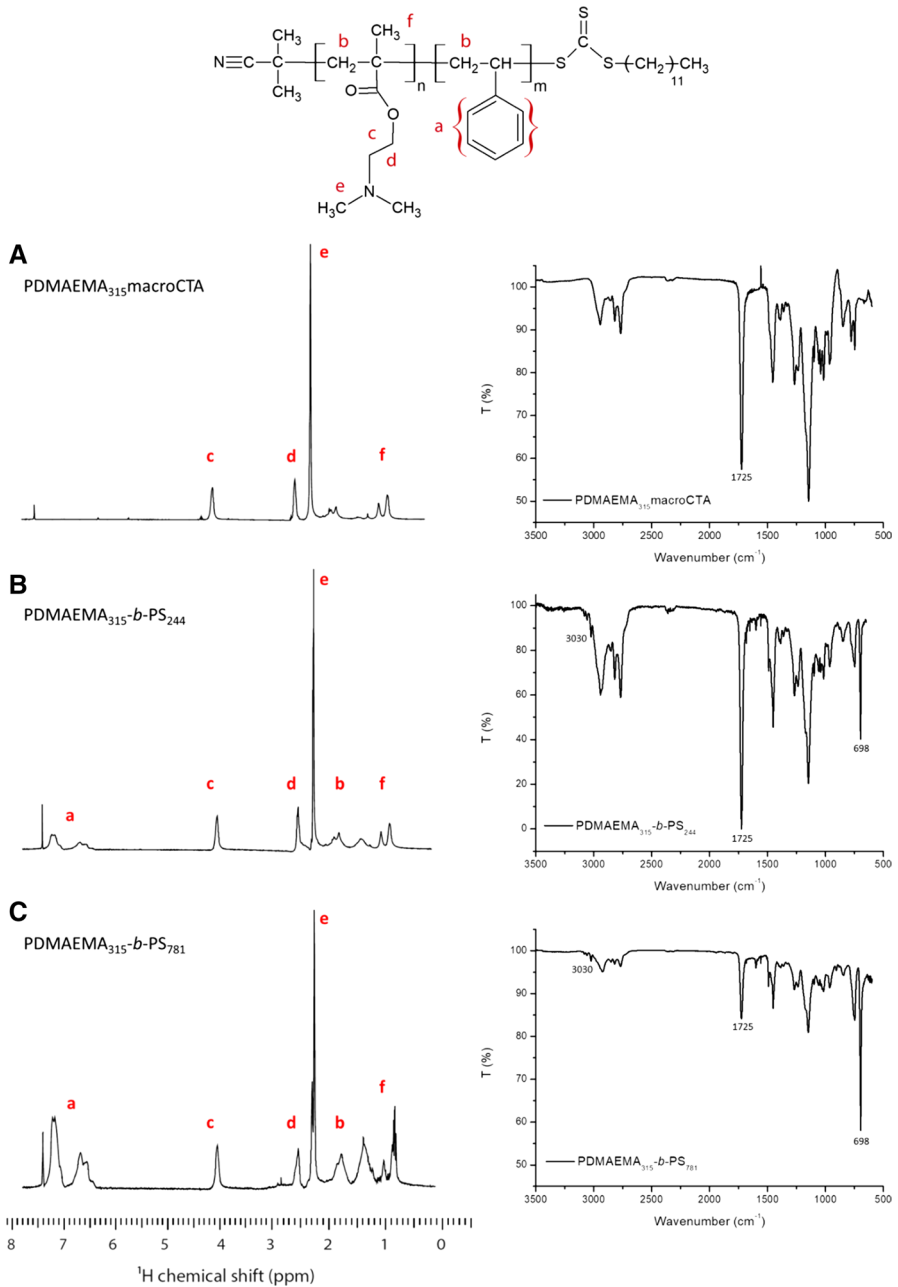


Fig. 3 ¹H-NMR (left) and FTIR results spectra (right) of **a** PDMAEMA₃₁₅macroCtA, **b** PDMAEMA₃₁₅-*b*-PS₂₄₄ and **c** PDMAEMA₃₁₅-*b*-PS₇₈₁. NMR peaks were assigned (letters a–f). The peaks used to confirm the copolymerization by FTIR are indicated in the IR spectra

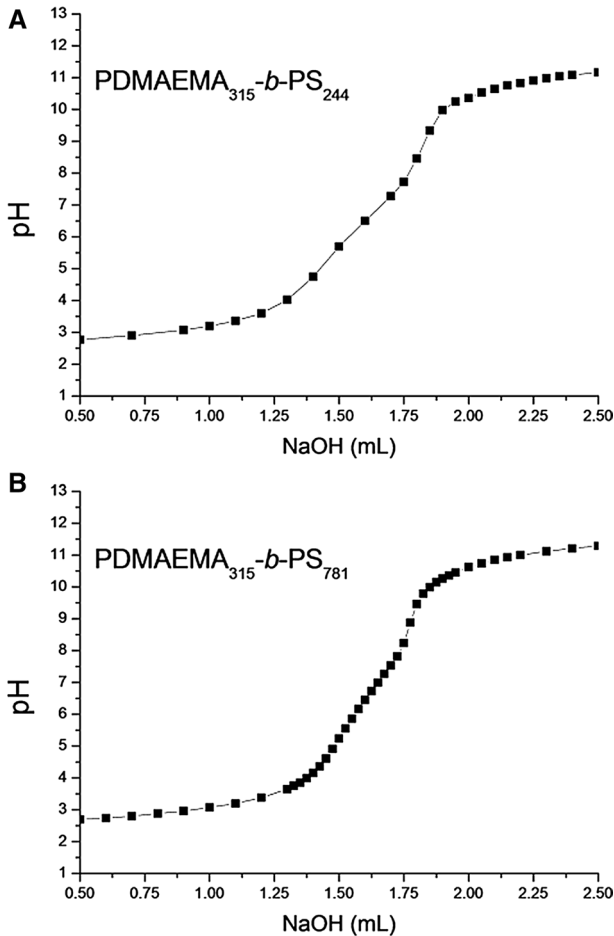


Fig. 4 Titration curves of the copolymers **a** PDMAEMA₃₁₅-*b*-PS₂₄₄ and **b** PDMAEMA₃₁₅-*b*-PS₇₈₁. PDMAEMA 315 -*b*-PS 244 (0.0030 g) and PDMAEMA 315 -*b*-PS 781 (0.0061 g) in THF were added, under stirring, to the HCl solution. The final % THF was 0.4%

corresponding to the total dissociation of the amino groups of PDMAEMA (Fig. 4). Both copolymers exhibited a wide pH dissociation range, at pH values lower than that of the DMAEMA monomer (pK_a 8.3) [58]. The pH range where the cationic chain of the copolymers dissociated is between 4.74 and 8.46 for PDMAEMA₃₁₅-*b*-PS₂₄₄ (mean pK_a of 6.60) and between 4.91 and 8.23 for PDMAEMA₃₁₅-*b*-PS₇₈₁ (mean pK_a of 6.57). As previously reported, regarding the ionization state of PDMAEMA diblock copolymers, both copolymers' mean pK_a was ca. 1.5 pH units lower than that of the monomer [43]. The interdependence of the amino groups close together in the same polymer chain explains both the lower pK_a (as compared to the monomer) and the wider dissociation range [43]. In addition, the size of the

hydrophobic PS block of PDMAEMA-*b*-PS did not modify the copolymers' mean pKa.

Polymeric vesicles assembly and characterization

Hydrodynamic diameter and zeta potential of the polymersomes—dynamic light scattering

The average hydrodynamic diameters (number average, nm) and size distribution (polydispersity index, PDI) of the polymersomes, prepared with different buffers and pHs, were measured by DLS (Table 2). The average hydrodynamic diameter values presented in Table 2 were calculated from the number distribution of particles of each size ("Experimental" section). The aggregates formed by both polymers showed hydrodynamic diameters ranging from 58 nm (PDMAEMA₃₁₅-*b*-PS₇₈₁ Tris-HCl pH 8.0) to 147 nm (PDMAEMA₃₁₅-*b*-PS₂₄₄, Tris-HCl, pH 7.4), consistent with the expected size of vesicles, suggesting that these copolymers assembled into polymersomes in aqueous buffer solution.

The zeta potential of the aggregates formed by both the copolymers decreased from ca. +44 mV to ca. +12 mV with increasing pH, a result compatible with amine deprotonation (Table 2). The length of the hydrophobic PS block did not affect the pH effect on the Zeta potential significantly in good agreement with the titration results (see above) (Fig. 4). Zeta potential values of both copolymers at pH 8.0 in phosphate buffer, however, were appreciably lower than those obtained at the same pH in Tris-HCl buffer (Table 2). Phosphate anion may bind to the copolymers more efficiently than Cl⁻, as observed in a variety of other self-aggregated structures [59].

As the pH increases from 5.0 to 8.0, the PDMAEMA block becomes less charged, due to ammonium deprotonation, decreasing the repulsion between the segments of hydrophilic chains. The change in the ionization state of the amino groups with increasing pH can trigger a decrease in the hydrodynamic diameter of the polymersomes, since the decrease in charge/charge repulsion can allow tighter packing of the repetitive units of PDMAEMA, leading to less stretched chains.

As the pH increases, the hydrophilic corona becomes thinner due to the decrease in self-repulsion [20–22, 55]. This effect was observed for the polymersomes of both copolymers. The size comparison only makes sense for the same buffer (same counterion). PDMAEMA₃₁₅-*b*-PS₂₄₄ size drops 41% going from pH = 7.4 to 8.0. PDMAEMA₃₁₅-*b*-PS₇₈₁ size decrease was 28% for the same pH change (Table 2). Such differences are probably related to multiple factors, including the average number of unimers in each aggregate and the hydrophilic/hydrophobic ratio of the copolymers [16].

PDMAEMA copolymers usually present a lower critical solution temperature (LCST) at which the interaction of the hydrophilic groups with water decreases, turning them insoluble [20, 21, 55]. For PDMAEMA-based polymers LCST occurs at lower temperatures for higher pH's. Above LCST, the copolymer is insoluble, mainly because the entropic component of the solubilization process becomes more significant than the enthalpic component, resulting in a positive solubilization ΔG

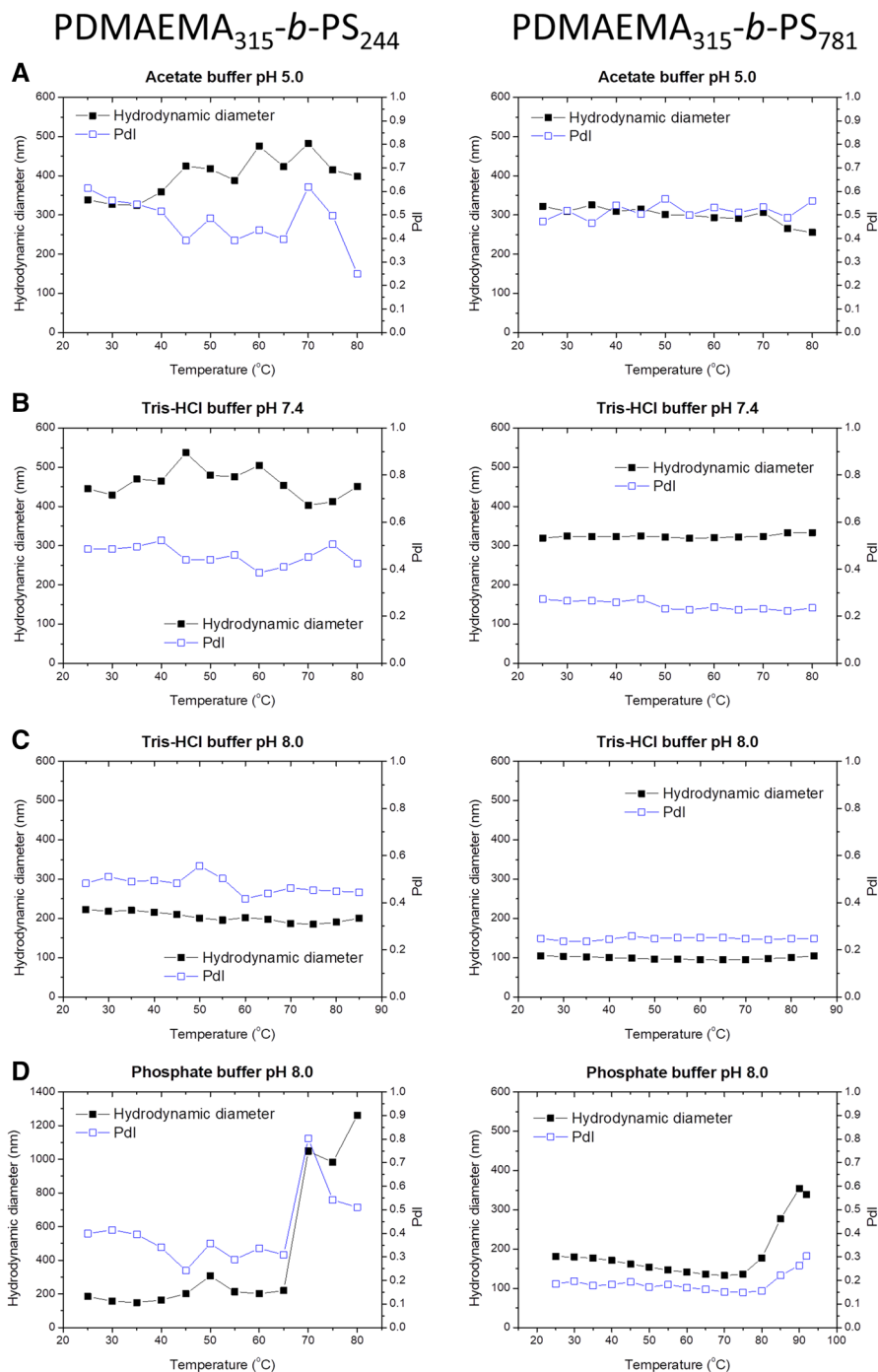


Fig. 5 Hydrodynamic diameter (size scatter average, D_h) and polydispersity index (PDI) of polymersomes as a function of temperature, at different pH and buffers (0.01 mol L⁻¹). **a** Acetate, pH 5.0; **b** Tris-HCl, pH 7.4; **c** phosphate, pH 8.0; **d** Tris-HCl, pH 8.0

value for the corona. This effect is determined mainly by hydrogen bond interactions (or not) between the solvent and the polymer functional group [20].

LCST of the polymersomes were studied by increasing the temperature from 25 °C to 85 °C and measuring the hydrodynamic diameter, calculated from the scatter intensity of each particle, leading to a size-averaged diameter, as described in the "Experimental" section, in opposition to the number average presented previously. By considering the hydrodynamic diameter, calculated from the scatter intensity distribution, one should note that the values differ from those presented at Table 2. The hydrodynamic diameter calculated from the scatter distribution is used here to monitor overall changes in particle size because the larger particles have more impact on the average.

No significant change on the average size of the vesicles was observed at the three pH values for acetate and Tris–HCl buffers for both copolymers in all temperature range studied (Fig. 5). For phosphate buffer at pH=8.0, as the temperature increased, an increase in the hydrodynamic diameter and polydispersity index of polymersomes of PDMAEMA₃₁₅-*b*-PS₂₄₄ and PDMAEMA₃₁₅-*b*-PS₇₈₁ was observed at 65 °C and 85 °C, respectively (Fig. 5). Nucleation and conformational effects of phosphate on polyamines have been recently described and may account for this effect [60]. The surface charge density also affects the temperature transition since, in more positively charged surfaces, the magnitude of the water-copolymer interactions (ion–dipole) is larger when compared to less charged surfaces at the same temperature. Surface hydration could explain the LCST effects observed for samples prepared in phosphate buffer that present lower Zeta potentials (Table 2), and are not observed in samples prepared in Tris–HCl buffer in which polymersomes present higher Zeta potential. Since LCST is the temperature in which both enthalpic and entropic contributions to solubilization are equal, a greater enthalpic contribution, in a process with (the same) negative entropy variation, leads to the LCST to be at a higher temperature.

The behavior reported here confirms that polymersomes of PDMAEMA-*b*-PS respond both to pH and temperature, and to other factors, such as the type of buffer and the anions present. All those variables can be combined to tailor systems based on this material that undergo precipitation at a particular temperature, pH or the presence of a specific kind of salt.

An internal aqueous compartment in the polymersomes

Evidencing the existence of an internal aqueous compartment is crucial for the demonstration of the existence of a closed vesicle-like aggregate. To verify the presence of an internal aqueous compartment in the polymeric aggregates, we prepared polymersomes in a solution of CAT1, a cationic and hydrophilic EPR probe. EPR signals of the sample before and after the addition of ascorbate in the bulk solution were measured (Fig. 6) [61]. Ascorbate reacts with the probe quenching its EPR signal (transferring of the unpaired electron to ascorbate). The residual signal after ascorbate reduction of CAT1 in the external aqueous phase was ascribed to the entrapped spin probe (See "Methods" section, Fig. 6, inset).

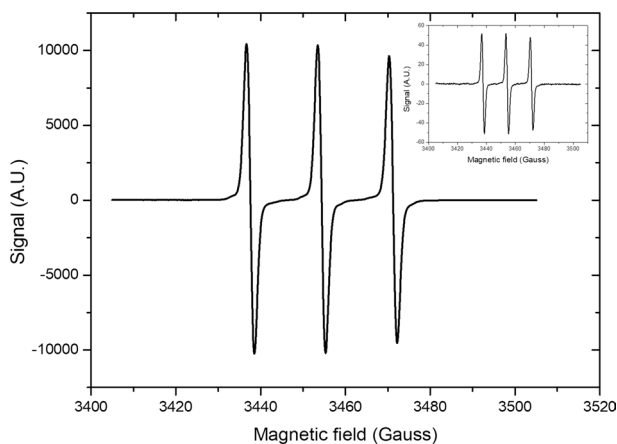


Fig. 6 EPR spectrum of CAT1 in a suspension of PDMAEMA₃₁₅-*b*-PS₇₈₁ polymersomes before and after (inset) addition of ascorbate. Polymersomes were prepared at 1 mg ml⁻¹, in Tris–HCl 10 mol L⁻¹ pH 7.4, CAT1 1.5 mmol L⁻¹. Final concentration of ascorbic acid was of 2.35 mmol L⁻¹

Table 3 EPR total and residual signals before and after ascorbate addition, percentage of entrapment, and total aqueous compartment volume of 1 mg mL⁻¹ solution of PDMAEMA₃₁₅-*b*-PS₂₄₄ and PDMAEMA₃₁₅-*b*-PS₇₈₁ polymersomes

Sample	Total EPR signal ($\times 10^{-3}$)	Residual EPR signal ($\times 10^{-3}$)	% of entrapment	Polymersomes total internal volume (μL)
Control	2.816	Not detectable	–	–
PDMAEMA ₃₁₅ - <i>b</i> -PS ₂₄₄	2.790	0.0163	0.59 \pm 0.07	1.00
PDMAEMA ₃₁₅ - <i>b</i> -PS ₇₈₁	2.706	0.0143	0.53 \pm 0.05	0.90

The calculated percentages of entrapment were 0.59 and 0.53% of samples' total volume for PDMAEMA₃₁₅-*b*-PS₂₄₄ and PDMAEMA₃₁₅-*b*-PS₇₈₁ polymersomes, respectively, at a final concentration of 1 mg of the copolymer in 1 mL solution (Table 3). These results demonstrated the presence of an internal aqueous compartment, impermeable to both CAT1 and ascorbate.

The degree of encapsulation of the EPR probe measured for both polymersomes preparations is in agreement with calculations considering particle radius, polymer concentration, molecular weight, and area per molecule [62]. Taking extruded polymersomes with a diameter of 400 nm and sharp size distribution, we estimate, for a 1 mg mL⁻¹ polymersome suspension, an entrapment percentage of ca. 0.45% [62].

Size distribution and morphology of polymersomes by TEM

Negative staining-TEM of the polymersomes formed in water showed the presence of spherical aggregates resembling a vesicle bearing an internal hydrophilic compartment isolated from bulk solution by a polymeric continuous layer (Figs. 7 and 8).

Images in Figs. 7a, b and 8a, b show aggregates of different diameters, but, as the aggregates may be in different depth planes in the grid, the degree of polydispersity may be lower than that in the image. Due to this fact, statistical analysis of polymersomes average diameter and size distribution was performed considering the contrast level of the observable polymer vesicles. PDMAEMA₃₁₅-*b*-PS₂₄₄ and PDMAEMA₃₁₅-*b*-PS₇₈₁ polymersomes have diameters of 74 ± 18 nm ($n = 18$) and

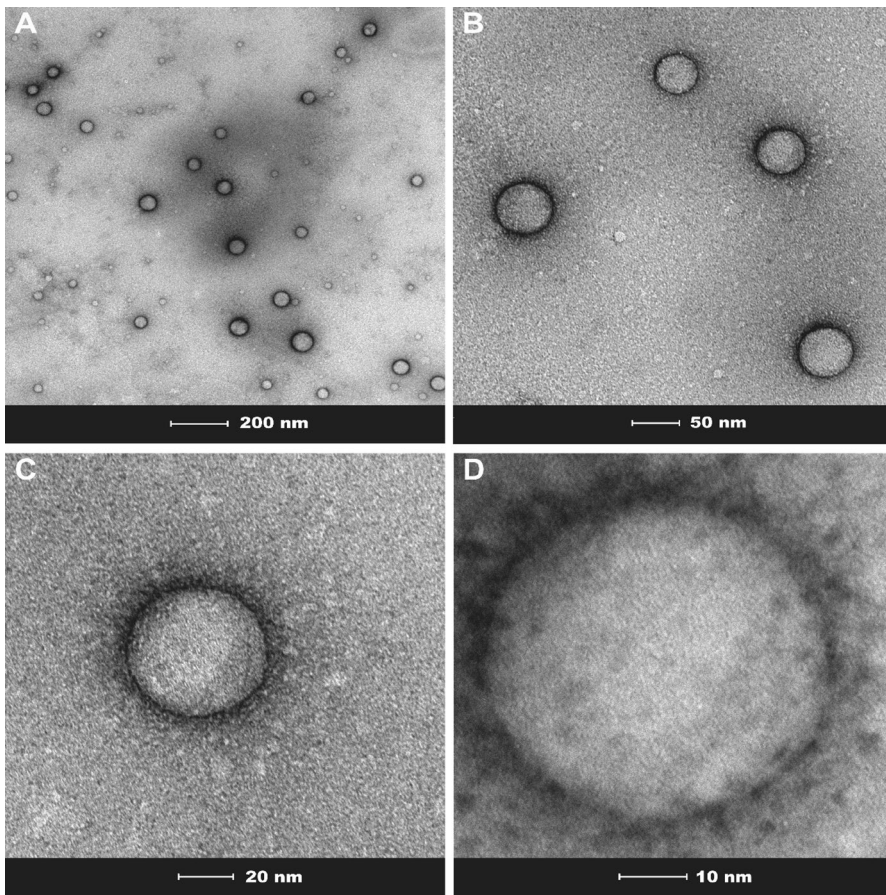


Fig. 7 Negative staining-TEM images of polymersomes of PDMAEMA₃₁₅-*b*-PS₂₄₄ assembled in 10 mmol L⁻¹ Tris-HCl buffer (pH 7.4). **a–d** Correspond to different places of the grid and magnification. The bar on the bottoms of each micrograph serves as size reference

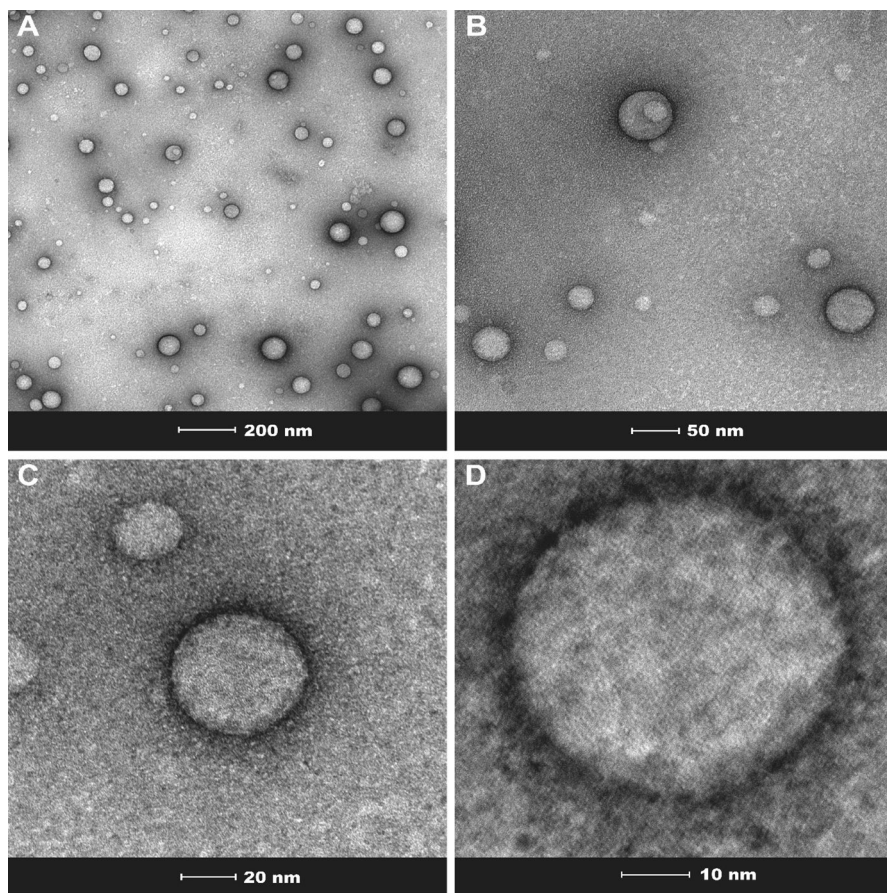


Fig. 8 Negative staining-TEM images of polymersomes of PDMAEMA₃₁₅-b-PS₇₈₁ assembled in 10 mmol L⁻¹ Tris-HCl buffer (pH 7.4). **a–d** Correspond to different places of the grid and magnification. The bar on the bottoms of each micrograph serves as size reference

78 ± 24 nm ($n=23$), respectively, Figs. 7c, d, 8c, d, in agreement with data obtained by DLS (Table 2).

EPR and TEM results together strongly suggest that the polymersomes have an internal hydrophilic compartment, separated from the external hydrophilic bulk solution by an amphiphilic bilayer. The hydrophobic layer is formed by PS blocks and the hydrophilic layer by PDMAEMA, according to the schematic representation in Fig. 9.

The character of the inner and outer hydrophilic cores can make the polymersomes presented here interesting for gene delivery, because of the ability of the positively charged amino groups of PDMAEMA to complex DNA [48, 53]. Also, the structures formed by the copolymers have a hydrophilic inner compartment capable of entrapping water and, therefore, water-soluble substances, which makes them potential candidates for nanoreactors [63].

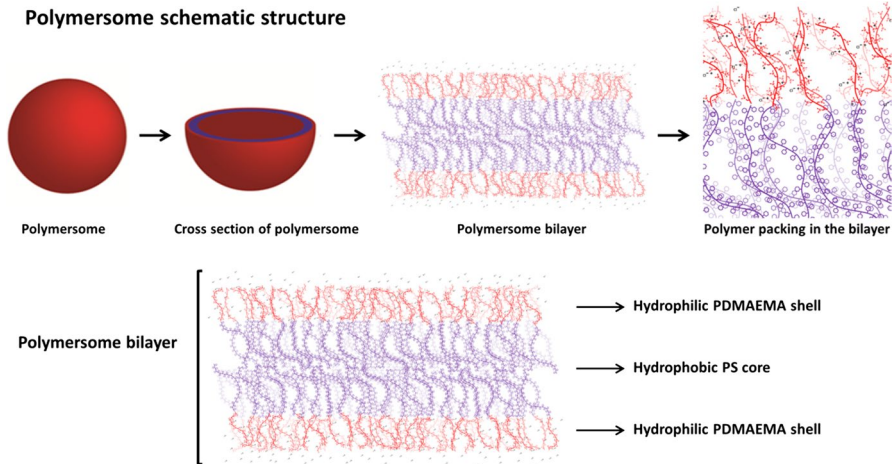


Fig. 9 Schematic representation of the suggested morphology of the polymersomes, supported by the DLS, EPR and negative staining-TEM data

Conclusions

Diblock copolymers of PDMAEMA-*b*-PS obtained via RAFT technique aggregate in aqueous solutions forming well-characterized multi-responsive polymersomes. pH, temperature and the type of buffer affect the aggregates’ size, indicating that the dissociation degree of the PDMAEMA amino group and the net charge of the corona are central for the structure and stability of the aggregates. Such variables may be used to generate tailored systems for numerous applications. EPR and negative staining-TEM analyses demonstrated that the aggregates are polymersomes with a hydrophilic inner core, impermeable to ascorbic acid and the cationic EPR probe CAT1. Among other potential applications, these polymersomes are potential platforms for nanoreactors and gene delivery.

Acknowledgements IMC, HC and FHF thanks to FAPESP (Proc. 2013/08166-5). IMC thanks the National Council for Scientific and Technological Development (CNPq – 465259/2014-6). IMC and HC thank the Coordination for the Improvement of Higher Education Personnel (CAPES), the National Institute of Science and Technology Complex Fluids (INCT-FCx) and NAP-FCx (Núcleo de Apoio à Pesquisa de Fluidos Complexos da Universidade de São Paulo). G.P.B.Carretero thanks the Programa CAPES: INCT -Institutos Nacionais de Ciência e Tecnologia (Proc. 88887.137085/2017-00) and FAPESP (2018/15230-5). FHF thanks CNPq (Universal 457733/2014-4), and GKVS acknowledges the Projeto Biocomputacional/CAPES (proc. no. 23038.004630/2014-35) and CNPq (proc. 457733/2014-4).

Funding Fundação de Amparo à Pesquisa do Estado de São Paulo—FAPESP (Grants 2013/08166–5 and 2018/15230–5). National Council for Scientific and Technological Development. CNPq (Grants 465259/2014–6 and 457733/2014–4). Coordination for the Improvement of Higher Education Personnel (CAPES). The National Institute of Science and Technology Complex Fluids (INCT-FCx) and NAP-FCx (Núcleo de Apoio à Pesquisa de Fluidos Complexos da Universidade de São Paulo). CAPES: INCT -Institutos Nacionais de Ciência e Tecnologia (Proc. 88887.137085/2017–00). Projeto Biocomputacional/CAPES (proc. no. 23038.004630/2014–35).

Compliance with ethical standards

Conflict of interest The authors declare that they have no conflict of interest.

Availability of data and material Data are available under request.

References

1. Che H, van Hest JCM (2016) Stimuli-responsive polymersomes and nanoreactors. *J Mater Chem B* 4:4632–4647. <https://doi.org/10.1039/C6TB01163B>
2. Hu X, Zhang Y, Xie Z et al (2017) Stimuli-responsive polymersomes for biomedical applications. *Biomacromol* 18:649–673. <https://doi.org/10.1021/acs.biomac.6b01704>
3. Agut W, Brûlet A, Schatz C et al (2010) pH and temperature responsive polymeric micelles and polymersomes by self-assembly of poly[2-(dimethylamino)ethyl methacrylate]-*b*-poly(glutamic acid) double hydrophilic block copolymers. *Langmuir* 26:10546–10554. <https://doi.org/10.1021/la1005693>
4. Pawar PV, Gohil SV, Jain JP, Kumar N (2013) Functionalized polymersomes for biomedical applications. *Polym Chem* 4:3160. <https://doi.org/10.1039/c3py00023k>
5. Yildirim T, Traeger A, Sungur P et al (2017) Polymersomes with endosomal pH-induced vesicle-to-micelle morphology transition and a potential application for controlled doxorubicin delivery. *Biomacromol* 18:3280–3290. <https://doi.org/10.1021/acs.biomac.7b00931>
6. Discher DE, Ahmed F (2006) Polymersomes. *Annu Rev Biomed Eng* 8:323–341
7. Wen J, Yuan L, Yang Y et al (2013) Self-assembly of monoterethered single-chain nanoparticle shape amphiphiles. *ACS Macro Lett* 2:100–106. <https://doi.org/10.1021/mz300636x>
8. Kozlovskaya V, Kharlampieva E (2020) Self-assemblies of thermoresponsive poly(*N*-vinylcaprolactam) polymers for applications in biomedical field. *ACS Appl Polym Mater* 2:26–39. <https://doi.org/10.1021/acscapm.9b00863>
9. Ren Y, Jiang X, Yin J (2008) Copolymer of poly(4-vinylpyridine)-*g*-poly(ethylene oxide) respond sharply to temperature, pH and ionic strength. *Eur Polymer J* 44:4108–4114. <https://doi.org/10.1016/j.eurpolymj.2008.09.025>
10. Neve A, Cantatore FP, Maruotti N, et al (2014) Extracellular matrix modulates angiogenesis in physiological and pathological conditions. In: *BioMed Research International*. <https://www.hindawi.com/journals/bmri/2014/756078/>. Accessed 21 Jul 2020
11. Glass L, Mackey MC (1979) Pathological conditions resulting from instabilities in physiological control systems*. *Ann N Y Acad Sci* 316:214–235. <https://doi.org/10.1111/j.1749-6632.1979.tb29471.x>
12. Obara M, Szeliga M, Albrecht J (2008) Regulation of pH in the mammalian central nervous system under normal and pathological conditions: facts and hypotheses. *Neurochem Int* 52:905–919. <https://doi.org/10.1016/j.neuint.2007.10.015>
13. Gupta P, Vermani K, Garg S (2002) Hydrogels: from controlled release to pH-responsive drug delivery. *Drug Discov Today* 7:569–579. [https://doi.org/10.1016/S1359-6446\(02\)02255-9](https://doi.org/10.1016/S1359-6446(02)02255-9)
14. Onaca O, Enea R, Hughes DW, Meier W (2009) Stimuli-responsive polymersomes as nanocarriers for drug and gene delivery. *Macromol Biosci* 9:129–139. <https://doi.org/10.1002/mabi.200800248>
15. Ward MA, Georgiou TK (2011) Thermoresponsive polymers for biomedical applications. *Polymers* 3:1215–1242. <https://doi.org/10.3390/polym3031215>
16. Discher DE, Ortiz V, Srinivas G et al (2007) Emerging applications of polymersomes in delivery: From molecular dynamics to shrinkage of tumors. *Prog Polym Sci* 32:838–857. <https://doi.org/10.1016/j.progpolymsci.2007.05.011>
17. Kita-Tokarczyk K, Grumelard J, Haefele T, Meier W (2005) Block copolymer vesicles—using concepts from polymer chemistry to mimic biomembranes. *Polymer* 46:3540–3563. <https://doi.org/10.1016/j.polymer.2005.02.083>
18. Leong J, Teo JY, Aakalu VK et al (2018) Engineering polymersomes for diagnostics and therapy. *Adv Healthc Mater* 7:1701276. <https://doi.org/10.1002/adhm.201701276>

19. Barrella MC, Capua AD, Adami R et al (2017) Impact of intermolecular drug-copolymer interactions on size and drug release kinetics from pH-responsive polymersomes. *Supramol Chem* 29:796–807. <https://doi.org/10.1080/10610278.2017.1377836>
20. de Souza JCP, Naves AF, Florenzano FH (2012) Specific thermoresponsiveness of PMMA-block-PDMAEMA to selected ions and other factors in aqueous solution. *Colloid Polym Sci* 290:1285–1291. <https://doi.org/10.1007/s00396-012-2651-9>
21. Lee H, Son SH, Sharma R, Won Y-Y (2011) A Discussion of the pH-Dependent Protonation Behaviors of Poly(2-(dimethylamino)ethyl methacrylate) (PDMAEMA) and Poly(ethylenimine-ran-2-ethyl-2-oxazoline) (PEI-r-EOz). *J Phys Chem B* 115:844–860. <https://doi.org/10.1021/jp109151s>
22. Xiong Z, Peng B, Han X et al (2011) Dual-stimuli responsive behaviors of diblock polyampholyte PDMAEMA-b-PAA in aqueous solution. *J Colloid Interface Sci* 356:557–565. <https://doi.org/10.1016/j.jcis.2011.01.067>
23. Oh J-M, Lee H-J, Shim H-K, Choi S-K (1994) Synthesis and surface activity of novel ABA type triblock cationic amphiphiles. *Polym Bull* 32:149–154. <https://doi.org/10.1007/BF00306381>
24. Xue Y, Wei D, Zheng A et al (2014) Study of stimuli-sensitivities of amphiphilic modified star poly[N,N-(dimethylamino)ethyl methacrylate] and its ability of DNA complexation. *J Macromol Sci A* 51:898–906. <https://doi.org/10.1080/10601325.2014.953374>
25. Arslan H, Zirtül O, Büttin V (2013) The synthesis and solution behaviors of novel amphiphilic block copolymers based on d-galactopyranose and 2-(dimethylamino)ethyl methacrylate. *Eur Polymer J* 49:4118–4129. <https://doi.org/10.1016/j.eurpolymj.2013.09.018>
26. Xiong Q, Ni P, Zhang F, Yu Z (2004) Synthesis and characterization of 2-(Dimethylamino)ethyl Methacrylate Homopolymers via aqueous RAFT polymerization and their application in miniemulsion polymerization. *Polym Bull* 53:1–8. <https://doi.org/10.1007/s00289-004-0308-7>
27. Zhang C, Maric M (2011) Synthesis of stimuli-responsive, water-soluble Poly[2-(dimethylamino)ethyl methacrylate/styrene] statistical copolymers by nitroxide mediated polymerization. *Polymers* 3:1398–1422. <https://doi.org/10.3390/polym3031398>
28. Zhu YJ, Tan YB, Du X (2008) Preparation and self-assembly behavior of polystyrene-block-poly(dimethylaminoethyl methacrylate) amphiphilic block copolymer using atom transfer radical polymerization. *Express Polym Lett* 2:214–225. <https://doi.org/10.3144/expresspolymlett.2008.26>
29. Song Y, Zhang T, Song X et al (2015) Polycations with excellent gene transfection ability based on PVP-g-PDMAEMA with random coil and micelle structures as non-viral gene vectors. *J Mat Chem B* 3:911–918. <https://doi.org/10.1039/c4tb01754d>
30. Zhu C, Jung S, Luo S et al (2010) Co-delivery of siRNA and paclitaxel into cancer cells by biodegradable cationic micelles based on PDMAEMA-PCL-PDMAEMA triblock copolymers. *Biomaterials* 31:2408–2416. <https://doi.org/10.1016/j.biomaterials.2009.11.077>
31. Moad G, Rizzardo E, Thang SH (2009) Living radical polymerization by the RAFT process: sa second update. *Aust J Chem* 62:1402. <https://doi.org/10.1071/CH09311>
32. Florenzano FH (2008) Perspectivas Atuais para a Obtenç\ ao Controlada de Polímeros e sua Caracterizaç\ ao. *Polímeros: Ciência e Tecnologia* 18:100–105
33. Mertoglu M (2005) The synthesis of well-defined functional homo-and block copolymers in aqueous media via Reversible Addition-Fragmentation Chain Transfer (RAFT) Polymerization. *Universidade de Postdam*
34. Stenzel MH (2008) RAFT polymerization: an avenue to functional polymeric micelles for drug delivery. *Chem Commun.* <https://doi.org/10.1039/b805464a>
35. Moad G, Thang SH (2009) RAFT polymerization: materials of the future, science of today: radical polymerization: the next stage. *Aust J Chem* 62:1379. <https://doi.org/10.1071/CH09549>
36. Rizzardo E, Chen M, Chong B, et al (2007) RAFT polymerization: adding to the picture. In: *Macromolecular symposia*. pp 104–116
37. Souza VV, Noronha MLdeC, Almeida FLA et al (2011) Cmc of PMMA-block-PDMAEMA measured by NPN fluorescence. *Polym Bull* 67:875–884. <https://doi.org/10.1007/s00289-011-0508-x>
38. Kim MR, Cheong IW (2016) Stimuli-triggered formation of polymersomes from W/O/W multiple double emulsion droplets containing poly(styrene)-block-poly(N-isopropylacrylamide-cospironaphthoxazine methacryloyl). *Langmuir* 32:9223–9228. <https://doi.org/10.1021/acs.langmuir.6b02178>
39. Kawahara N, Kojoh S, Matsuo S et al (2006) Synthetic method of polyethylene-poly(methylmethacrylate) (PE-PMMA) polymer hybrid via reversible addition-fragmentation chain

- transfer (RAFT) polymerization with functionalized polyethylene. *Polym Bull* 57:805–812. <https://doi.org/10.1007/s00289-006-0642-z>
40. Moore JC (1964) Gel permeation chromatography. I. A new method for molecular weight distribution of high polymers. *J Polym Sci A: Gener Paper* 2:835–843. <https://doi.org/10.1002/pol.1964.100020220>
 41. Shen, (2012) Preparation and characterization of PMMA and its derivative via RAFT technique in the presence of disulfide as a source of chain transfer agent. *J Memb Separ Tech*. <https://doi.org/10.6000/1929-6037.2012.01.02.6>
 42. Ma S, Xiao M, Wang R (2013) Formation and structural characteristics of thermosensitive multi-block copolymer vesicles. *Langmuir* 29:16010–16017. <https://doi.org/10.1021/la404157h>
 43. Saraiva GKV, de Souza VV, Coutinho de Oliveira L et al (2019) Characterization of PMMA-b-PDMAEMA aggregates in aqueous solutions. *Colloid Polym Sci* 297:557–569. <https://doi.org/10.1007/s00396-019-04482-w>
 44. Lim Soo P, Eisenberg A (2004) Preparation of block copolymer vesicles in solution. *J Polym Sci B Polym Phys* 42:923–938. <https://doi.org/10.1002/polb.10739>
 45. Rauckman EJ, Rosen GM, Abou-Donia MB (1976) Synthesis of a useful spin labeled probe, 1-oxyl-4-carboxyl-2,2,6,6-tetramethylpiperidine. *J Org Chem* 41:564–565. <https://doi.org/10.1021/jo00865a037>
 46. Farkuh L, Hennies PT, Nunes C et al (2019) Characterization of phospholipid vesicles containing lauric acid: physicochemical basis for process and product development. *Heliyon*. <https://doi.org/10.1016/j.heliyon.2019.e02648>
 47. Schacher F, Rudolph T, Wieberger F et al (2009) Double stimuli-responsive ultrafiltration membranes from polystyrene-block-poly(*N,N*-dimethylaminoethyl) symers. *ACS Appl Mater Interfaces* 1:1492–1503. <https://doi.org/10.1021/am900175u>
 48. Liu Q, Yu Z, Ni P (2004) Micellization and applications of narrow-distribution poly[2-(dimethylamino)ethyl methacrylate]. *Colloid Polym Sci* 282:387–393. <https://doi.org/10.1007/s00396-003-0956-4>
 49. Chen J, Liu M, Gong H et al (2013) Synthesis of linear amphiphilic tetrablock quaterpolymers with dual stimulus response through the combination of ATRP and RAFT by a click chemistry site transformation approach. *Polym Chem* 4:1815–1825. <https://doi.org/10.1039/C2PY20946B>
 50. Tang J, Lee MFX, Zhang W et al (2014) Dual responsive pickering emulsion stabilized by poly[2-(dimethylamino)ethyl methacrylate] grafted cellulose nanocrystals. *Biomacromol* 15:3052–3060. <https://doi.org/10.1021/bm500663w>
 51. Yanez-Macias R, Alvarez-Moises I, Perevyazko I et al (2017) Effect of the degree of quaternization and molar mass on the cloud point of poly[2-(dimethylamino)ethyl methacrylate] aqueous solutions: a systematic investigation. *Macromol Chem Phys* 218:1700065. <https://doi.org/10.1002/macp.201700065>
 52. Manganiello MJ, Cheng C, Convertine AJ et al (2012) Diblock copolymers with tunable pH transitions for gene delivery. *Biomaterials* 33:2301–2309. <https://doi.org/10.1016/j.biomaterials.2011.11.019>
 53. van de Wetering P, Cherng J-Y, Talsma H et al (1998) 2-(dimethylamino)ethyl methacrylate based (co)polymers as gene transfer agents. *J Control Release* 53:145–153. [https://doi.org/10.1016/S0168-3659\(97\)00248-4](https://doi.org/10.1016/S0168-3659(97)00248-4)
 54. Emileh A, Vashghani-Farahani E, Imani M (2007) Swelling behavior, mechanical properties and network parameters of pH- and temperature-sensitive hydrogels of poly((2-dimethyl amino) ethyl methacrylate-co-butyl methacrylate). *Eur Polymer J* 43:1986–1995. <https://doi.org/10.1016/j.eurpolymj.2007.02.002>
 55. Yıldız B, Işık B, Kış M, Birgül Ö (2003) pH-sensitive dimethylaminoethyl methacrylate (DMAEMA)/acrylamide (AAm) hydrogels: synthesis and adsorption from uranyl acetate solutions. *J Appl Polym Sci* 88:2028–2031. <https://doi.org/10.1002/app.11709>
 56. Cotanda P, Wright DB, Tyler M, O'Reilly RK (2013) A comparative study of the stimuli-responsive properties of DMAEA and DMAEMA containing polymers. *J Polym Sci, Part A: Polym Chem* 51:3333–3338. <https://doi.org/10.1002/pola.26730>
 57. Han X, Zhang X, Zhu H et al (2013) Effect of composition of PDMAEMA-b-PAA block copolymers on their ph- and temperature-responsive behaviors. *Langmuir* 29:1024–1034. <https://doi.org/10.1021/la3036874>

58. van de Wetering P, Moret EE, Schuurmans-Nieuwenbroek NME et al (1999) Structure–activity relationships of water-soluble cationic methacrylate/methacrylamide polymers for nonviral gene delivery. *Bioconjugate Chem* 10:589–597. <https://doi.org/10.1021/bc980148w>
59. Luo T, Abdu S, Wessling M (2018) Selectivity of ion exchange membranes: a review. *J Membr Sci* 555:429–454. <https://doi.org/10.1016/j.memsci.2018.03.051>
60. Andreozzi P, Ricci C, Porcel JEM et al (2019) Mechanistic study of the nucleation and conformational changes of polyamines in presence of phosphate ions. *J Colloid Interface Sci* 543:335–342. <https://doi.org/10.1016/j.jcis.2019.02.040>
61. Aracava Y, Schreier S, Phadke R et al (1981) Spin label reduction kinetics, a procedure to study the effect of drugs on membrane-permeability—the effects of monosodium urate, dimethylsulfoxide and amphotericin-B. *J Biochem Biophys Methods* 5:83–94. [https://doi.org/10.1016/0165-022X\(81\)90009-9](https://doi.org/10.1016/0165-022X(81)90009-9)
62. Stokes AM, Wilson JW, Warren WS (2012) Characterization of restricted diffusion in uni- and multi-lamellar vesicles using short distance iMQCs. *J Magn Reson* 223:31–40. <https://doi.org/10.1016/j.jmr.2012.07.021>
63. Zhu Y, Yang B, Chen S, Du J (2017) Polymer vesicles: Mechanism, preparation, application, and responsive behavior. *Prog Polym Sci* 64:1–22. <https://doi.org/10.1016/j.progpolymsci.2015.05.001>

Publisher's Note Springer Nature remains neutral with regard to jurisdictional claims in published maps and institutional affiliations.